Available online at www.sciencedirect.com
ScienceDirect
Nuclear Instruments and Methods in Physics Research B 258 (2007) 155–158
NIM B Beam Interactions with Materials & Atoms
www.elsevier.com/locate/nimb

Two-dimensional images of transmitted slow neon ions guided by nanocapillaries in polymer foils

Y. Kanai [a,*], M. Hoshino [b], T. Kambara [a], T. Ikeda [a], R. Hellhammer [c], N. Stolterfoht [c], Y. Yamazaki [a,d]

[a] *RIKEN, Wako, Saitama 351-0198, Japan*
[b] *Department of Physics, Sophia University, Chiyoda, Tokyo 102-8554, Japan*
[c] *Hahn-Meitner-Institut Berlin, Glienickerstrasse 100, D-14109 Berlin, Germany*
[d] *Institute of Physics, University of Tokyo, Meguro, Tokyo 153-8902, Japan*

Available online 22 December 2006

Abstract

We have measured two-dimensional images of 3.5–7 keV Ne^{7+} ions guided by PET nanocapillaries as a function of the deposited charge. The transmitted ion position and shape are found to change with the intensity evolution. After saturation of the guided ion intensity, the transmission profile is nearly isotropic and its angular width amounts to about 1°, which differs from previous measurements.

PACS: 34.50.Fa; 32.80.Fb

Keywords: Nanocapillary; PET polymer; Highly charged ions; Guiding effect

1. Introduction

Interactions between slow highly charged ions (HCIs) and solid surfaces have extensively been studied [1–3]. For HCI metal–surface interactions, especially charge transfer processes from the metallic surface, can be explained by the so called classical over the barrier model [4]. With a metallic microcapillary target, experimental evidence of hollow ions in vacuum and the detailed study of charge transfer processes have been demonstrated [5,6]. On the other hand, interactions between ions and insulator surface have more complicated features, which depend on the insulator surface properties [1,2]. Recently, Stolterfoht et al. [7] have shown that mesoscopic properties of insulator surfaces can be used to guide slow ions along the axis of an insulator nanocapillary. Qualitatively, this phenomenon can be explained as follows: (1) ions collide with the inner surface of a nanocapillary, which is charging up positively, (2) the following ions are deflected by the positively charged up surface into the capillary axis direction, (3) a great deal of the ions can be transmitted through insulator nanocapillaries without any close collisions with surface. Up to now, almost all experiments studying beam guiding effects have been done by measuring the guided ions with an electrostatic analyzer [7–10], where the energy and angular distributions of the transmitted ions were measured by changing the analyzer voltage and position. With such measurements, it is rather difficult to measure spatial profile changes of the transmitted ions, which change sometimes within a few seconds. Therefore, we utilized a two-dimensional (2-D) detector to measure the transmitted ions. Moreover we used a new polyethylene terephthalate (PET) sample with parallel capillaries of low density (4×10^6 capillaries/cm^2) as target to reduce the total number of transmitted ions to values less than 10,000 s^{-1} while keeping incident ion-currents for each capillary (0.1–10 ions/capillary/s) the same as used in the previous studies

* Corresponding author. Tel.: +81 48 467 9486; fax: +81 48 462 4644.
E-mail address: kanaiyasuyuki@riken.jp (Y. Kanai).

0168-583X/$ - see front matter © 2006 Elsevier B.V. All rights reserved.
doi:10.1016/j.nimb.2006.12.090

[7]. The position information at the 2-D detector and the time information were recorded using a list mode. This method allows us to measure not only the evolution of transmitted ion intensity but also the spatial profile (position and shape) as a function of integrated ion current (i.e. the deposited charge Q), which reveals the time evolution of the charging up of the inner capillary surface.

2. Experiment

We performed the experiments at RIKEN with Ne^{7+} ions from a 14.5 GHz ECR ion source. The beam energies were 3.5–7 keV, and beam intensities 0.5–200 pA at the target position. Typical beam divergence was better than 0.5°. Size of the beam at the target was 1–1.5 mm in diameter. Experimental setup is shown in Fig. 1. The vacuum in the chamber was better than 1×10^{-5} Pa. 2-D detector, which consisted of MCPs and wedge and strip anode, was rotatable on the horizontal plane around the target (θ-direction). An electrostatic deflector was set just after the target position, when we needed to measure the charge state distribution of the transmitted ions.

A PET foil was attached at the target holder and was rotated by the angles θ and ϕ as shown in Fig. 1. The PET foil of 10 μm thickness was previously irradiated by 250 MeV Kr ions. Using NaOH for chemical etching of the ion tracks we produced capillaries with a diameter of 200 nm. The capillary density was 4×10^6 capillaries/cm^2, which was two orders of magnitude smaller than that of the target used for previous measurements [7]. To avoid a macroscopic charging up the surface of the PET foil, Au was evaporated on the front and exit sides. The position information at the 2-D detector, the time, and ion currents measured by the PET foil were recorded by a PC program working in list mode.

3. Results

Fig. 2 shows a typical intensity evolution with the integrated ion current Q caused by the guiding effects. Here, the tilt angles were $\theta = 2°$ and $\phi = -1°$, which were changed from the previous angles $\theta_0 = 2°$ and $\phi_0 = 1°$. Fig. 3

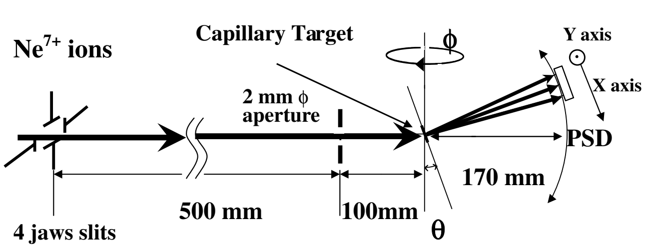

Fig. 1. Experimental setup. Ne^{7+} ions are collimated by 4 jaws-slits and a 2 mm ϕ aperture before the target, which can be rotated to the θ and ϕ directions as indicated. Transmitted ions are measured by a 2-D position sensitive detector (PSD). An electrostatic deflector can be set just after the target for analyzing the charge state of the transmitted ions.

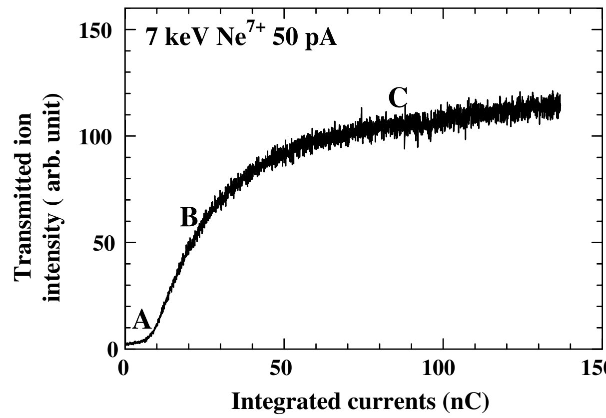

Fig. 2. Intensity evolution of 7 keV Ne^{7+} ions. The capillary target was set at the angles $\theta = 2°$ and $\phi = -1°$ from the previous angles $\theta_0 = 2°$, $\phi_0 = 1°$. A, B and C indicate the ranges corresponding to the 2-D images in Fig. 3.

shows 2-D images of the transmitted ions for different charges $Q = 0$–5 nC, 20–25 nC and 80–85 nC, acquired during the intensity evolution shown in Fig. 2. The contours are drawn in logarithmic scales. In this measurement, we resolved the charge states of the transmitted ions. Expected positions for neutral Ne and Ne^{7+} ions are shown as arrows in Fig. 3. At first ($Q = 0$–5 nC), a Ne atom peak and a weak Ne^{7+} ion peak were observed. The number of Ne^{7+} ions increased with increasing Q. The peak position of Ne^{7+} ions moved along the Y direction, to which the capillary was tilted from the previous measurement (ϕ–ϕ_0 direction). The direction of the peak shift was always along the direction to which the capillary was tilted from the previous measurement and may be attributed to a memory effect (influence of the charge distribution at the inner capillary wall produced by the previous experiment).

During the intensity evolution, the shape of the transmitted ion profile changed and sometimes was elongated along the direction to which the capillary was tilted from the previous measurement. After the saturation of the transmitted ion intensity, the shape was rather circular and the angular width was about 1°. Fig. 4 shows 2-D images of the transmitted ions after saturation for different tilt angle using 3.5 keV and 7 keV Ne^{7+} ions. The contours are drawn in linear scales. All 2-D images after the intensity saturation are rather circular and the angular width amounts to values from 1 to 1.5°. The angular widths for 3.5 keV are larger than those for 7 keV. This is consistent with previous measurements reported by Hellhammer et al. [8] who found that the lower the beam energy the wider is the angular width. However, the absolute angular widths of the transmitted ions of present experiments are much smaller than those reported in previous measurements [7–9]. This finding may be due to the difference in the capillary density. The present results are in good agreement with theoretical simulation [11], the results for SiO_2 capillaries [10], and for low density PET capillaries [12]. To discuss the relation between the capillary density and

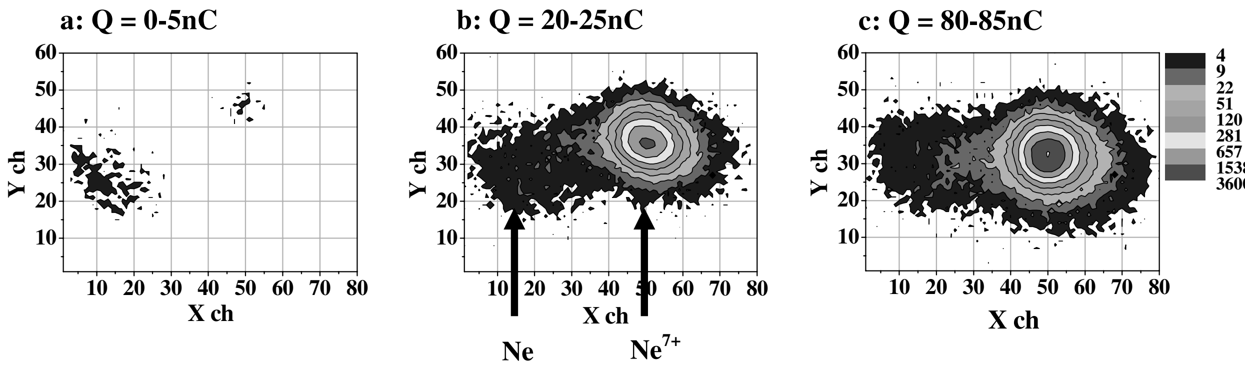

Fig. 3. 2-D images of transmitted ions during the intensity evolution in Fig. 2 for $Q = 0$–5 nC, 20–25 nC and 80–85 nC. Contours are plotted in logarithmic scales to see the weak intensities. The transmitted ion peak position moved along the Y axis, which corresponds to the ϕ–ϕ_0 direction. The charge states of transmitted ions were analyzed by an electrostatic deflector and the expected positions for Ne and Ne^{7+} are indicated by arrows. In the figure, 11 channels correspond to about 1°.

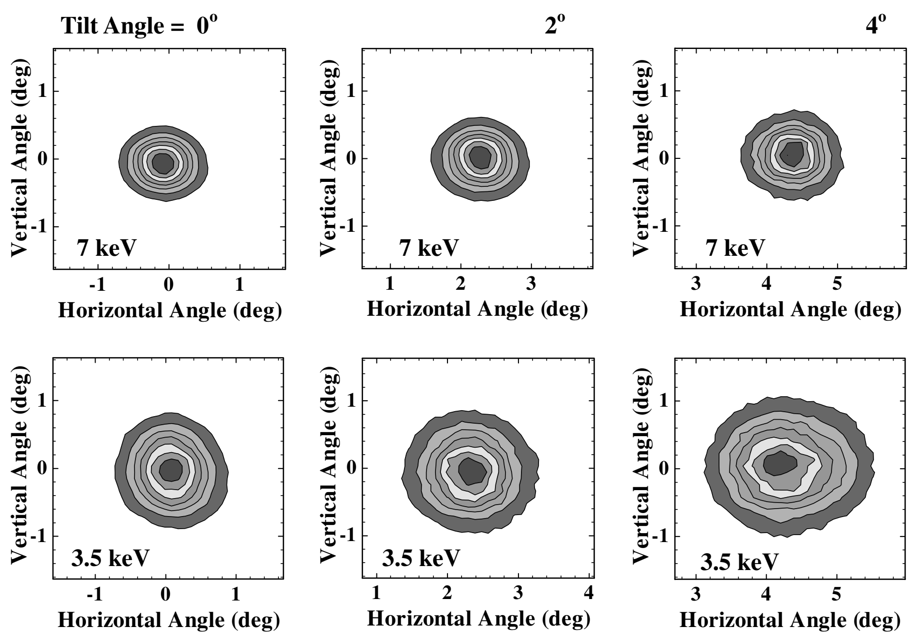

Fig. 4. 2-D images of transmitted 3.5 and 7 keV Ne^{7+} ions after intensity saturation for different tilt angles. The target was tilted to the θ direction and $\phi = 0°$ for all cases. The charge state of the transmitted ions was not analyzed. Contours are plotted in linear scales.

the angular width of guided ions, we need more detailed measurements by changing the capillary density.

4. Summary

The guided transmission of slow Ne^{7+} ions by PET capillaries with the density of 4×10^6 capillaries/cm^2 shows the following features; (1) during the evolution of the guided ion intensity, the position and shape of transmission profile change, which is due to the change of the charge distributions of inner capillary, (2) after saturation of the guided ion intensity, the angular width of transmitted ions are rather circular and with widths of 1–1.5° at FWHM. Further studies are needed to clarify the possible relation between the angular width of the guided ions and the capillary density.

Very recently, Ikeda et al. [13] observed the guiding effect for slow Ar^{8+} ions by a single tapered glass tube. It is a very interesting problem to study the relation of both guiding effects for nanocapillaries in PET foil and a single tapered glass tube.

References

[1] A. Arnau et al., Surf. Sci. Rep. 27 (1997) 113.
[2] T. Schenkel, A.V. Hamza, A.V. Barnes, D.H. Schneider, Prog. Surf. Sci. 61 (1999) 23.
[3] F.J. Currell (Ed.), The Physics of Multiply and Highly Charged Ions, Kluwer Academic Publishers, The Netherlands, 2003.

[4] J. Burgdörfer, P. Lerner, F.W. Meyer, Phys. Rev. A 44 (1991) 5674.
[5] S. Ninomiya, Y. Yamazaki, F. Koike, H. Masuda, T. Azuma, K. Komaki, K. Kuroki, M. Sekiguchi, Phys. Rev. Lett. 78 (1997) 4557.
[6] Y. Morishita et al., Phys. Rev. A 70 (2004) 012902.
[7] N. Stolterfoht, J.-H. Bremer, V. Hoffmann, R. Hellhammer, D. Fink, A. Petrov, B. Sulik, Phys. Rev. Lett. 88 (2002) 133201.
[8] R. Hellhammer, P. Sobocinski, Z.D. Pešić, J. Bundesmann, D. Fink, N. Stolterfoht, Nucl. Instr. and Meth. B 232 (2005) 235.
[9] Gy. Vikor, R.T. Rajendra Kumar, Z.D. Pešić, N. Stolterfoht, R. Schuch, Nucl. Instr. and Meth. B 233 (2005) 218.
[10] M.B. Sahana, P. Skog, Gy. Vikor, R.T. Rajendra Kumar, R. Schuch, Phys. Rev. A 73 (2006) 040901(R).
[11] K. Schiessl, W. Palfinger, K. Tökési, H. Nowotny, C. Lemell, J. Burgdörfer, Phys. Rev. A 72 (2005) 062902.
[12] R. Hellhammer, P. Sobocinski, D. Fink, J. Bundesman, B. Sulik, N. Stolterfoht, XXIVth ICPEAC, Abstracts (Rosario, Argentina, 2005) p. Tu129.
[13] T. Ikeda, Y. Kanai, T.M. Kojima, Y. Iwai, T. Kambara, Y. Yamazaki, M. Hoshino, T. Nebiki, T. Narusawa, App. Phys. Lett. 89 (2006) 163502.